# 23. *Anemometer of Inverted Pendulum Type and Wind Construction Studied with It.*

By Genrokuro NISHIMURA and Masazi SUZUKI,

Earthquake Research Institute.

(Read Dec. 19, 1940 and July 3, 1941.—Received June 30, 1954.)

## 1. Introduction.

At the occasion when we investigated the kaze-tsunami[1] caused by the Muroto Typhoon in 1934, we observed actually the damage done to Japanese wooden houses at Kansai District by this typhoon. At that time, the late Prof. M. Ishimoto, the director of the Earthq. Res. Inst., suggested to us that in order to clarify the relations between the damage[2] to houses and the blowing wind, it is necessary to study the wind constructions, and that in short time intervals such as one or two minutes. He also encouraged us, by making every effort to furnish the necessary funds, to take up the study of wind construction. Writing the present paper, we worship heartily the spirit of the late Prof. M. Ishimoto, and also pray for his happiness.

Now, we know that there are various types of anemometers such as Robinson's or Dynes', which are, however, not suitable for our purpose of studying the construction of natural wind. Therefore, we designed new a suitable anemometer which shall be shown in this paper. The present new-designed anemometer is of an inverted pendulum type, and it can actually catch the natural winds with variation periods equal to or longer than 0.1 sec. Moreover, by the present anemometer, we are able to obtain accurately the records of two components of the natural wind velocity which becomes equal to or smaller than 60 m/s.

The anemometer was installed on the roof of a Japanese ware-house which was situated in the neighbourhood of the sea coast of Inatori-machi, Izu Peninsula, Shizuoka Prefecture. The respective records of winds in the seasons of both spring and winter were obtained at the prescribed locality. The records of the winds of typhoon could not,

1) G. NISHIMURA and T. TAKAYAMA, *Bull. Earthq, Res. Inst., Suppl. Vol.*, **2** (1935).

2) The vibrations of a Japanese two-storied frame-house due to natural wind were also studied by us, and the mesurement of the wind pressure related to this study was done by the same anemometer described in the present paper.

G. NISHIMURA and M. SUZUKI, "Horizontal Deformations of a Japanese Two-Storied Frame-House," *Bull. Earthq. Res. Inst.*, **32** (1954).

however, be obtained in the course of observation by the present apparatus. Therefore, in this paper, we analysed the records obtained by the anemometer at the above-mentioned time, and obtained some interesting results concerning the wind constructions.

The present paper contains the following studies: (1) New-designed anemometer, (2) Time variation of wind pressure (Breath of wind pressure) and predominant periods of breath, (3) Breath and pressure of natural wind, and (4) Blowing direction and pressure of natural wind.

Of course, the present study of the natural winds is that of the winds at special locality and special observation times, and therefore the results obtained by the present analysis are not necessarily appropriate for the general study of the general characters of the natural winds. The present writers, however, hope that the present analysis will make a contribution to the study of the natural winds.

## 2. Theory and design of anemometer of inverted pendulum type.

We assume that the horizontal intensity of the pressure of the natural wind becomes $W$ kg-wt/cm$^2$, and the total horizontal pressure exerted on a sphere of which the outer diameter becomes $d$, is $W$ kg-wt. When the said sphere constructs an inverted pendulum as shown in Fig. 1, we can easily obtain the following equation of motion of the pendulum:

$$\frac{d^2\theta}{dt^2}+2\varepsilon\frac{d\theta}{dt}+\omega^2\theta=hW/I_0\,, \quad \cdots\cdots\cdots\cdots(1)$$

where $2\varepsilon=\lambda_0/I_0$, $\omega^2=K_0/I_0$, and $I_0$=the moment of inertia of the inverted pendulum about the rotation axis of the pendulum weight, $\lambda_0$=the constant related to the damping of the free vibration of the pendulum when the damping force becomes proportional to the rotation velocity $d\theta/dt$ of the pendulum, $K_0$=the restitutive moment of the pendulum, $h$=the distance between the rotation axis of the pendulum and the action point of the total pressure $W$ on the top sphere of the pendulum, and $\theta$, $t$, of course, show respectively the angle of rotation of the pendulum and the time of motion of the pendulum. Of course, in the present theory, the wind pressure $W$ is the force acting on the pendulum perpendicular to the axis of the pendulum and also works in the plane in which the pendulum's motion is constrained.

Now, assuming that the functional form $f(t)$ of the wind force $W$ becomes as follows:

(a) $W=f(t)=W_m(1-\cos \mu t)/2$ ,

(b) $W=f(t)=W_m \gamma t \cdot \exp(1-\gamma t)$ ,

(c) $W=f(t)=W_m \gamma^2 t^2/2 \cdot \exp(2-\gamma t)$ ,

(d) $W=f(t)=W_m \exp(-\gamma t) \cdot \sin \mu' t$ ,

(e) $W=f(t)=W_m\{1-\exp(-\gamma'' t)\}$ ,

we studied the characters of the pendulum motion. These expressions show respectively the different characters of the wind force with respect to time $t$, and we can easily obtain the solutions of the equation (1) for the respective five cases of $W$ shown in the expressions (a)~(e). In these expressions (a)~(e), the quantities such as $\mu$, $\mu'$, $\gamma$, $\gamma'$, $\gamma''$ having $[1/T]$ dimension are respectively the factors controlling both the sharpness and the acting time of the wind force. The analytical solutions of (1) corresponding to the respective cases of $W$ shown in the expressions (a)~(e) show that when the proper period of the inverted pendulum is made short and the damping force is not so large, the angle of the deflection of the pendulum $\theta$ coincides nearly with the amplitude $-f(t)/\omega^2$. The sensibility of the inverted pendulum, however, becomes inverse-proportional to the square of the natural period of it. And, therefore, when we make the period as short as possible, it is difficult to obtain a suitable mechanical magnification from the technical point of view. Of course, it is desirable to make the damping small to a certain degree, because when it becomes large, the phase-lag becomes large. But it is not desirable to make the damping too small, because the free vibration of

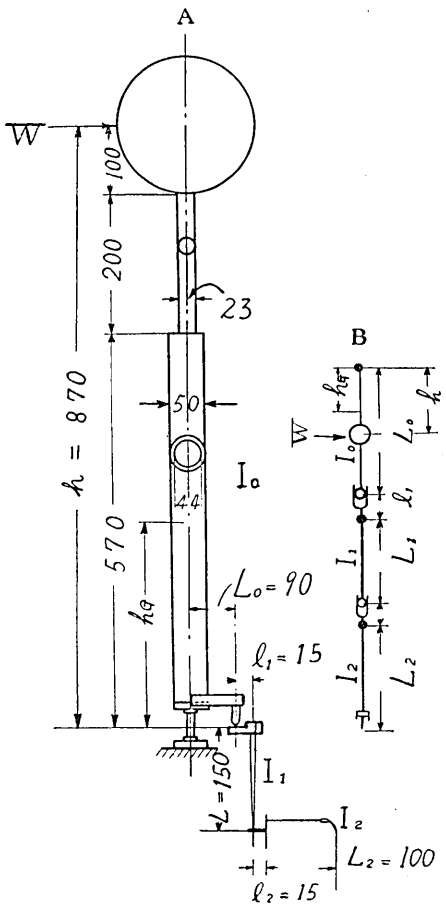


Fig. 1.

the inverted pendulum may be excited by the pressure of shock type of the natural wind.

Now, our object to obtain the wind variation with the anemometer is to catch the wind variation which becomes much effective on structures such as wooden houses or other tall towers. As a matter of fact, the free vibration periods of these structures are not very short as shown in the foot note[3]. Therefore, as we want to study the wind structures which are specially effective on the dynamical properties of the houses, buildings or towers, it is not desirable to make the natural period of the inverted pendulum, which is used for the main function body of the present new-designed anemometer, very short. Because, by this very short period of pendulum, the anemometer becomes of course sensible to the wind variation of very short periods which do not affect greatly the dynamical natures of vibration of the building. Thus, in order to obtain comparatively long variation of the period of natural wind pressure, the natural period of the inverted pendulum of the anemometer ought to be made comparatively long and to have a favourable damping for decreasing the sensitiveness to very short periodic variations due to winds of very short period. From these discussions, we determined both the period and the damping of the pendulum as follows: The natural period of the inverted pendulum $T_n=0.05$ sec.$\sim$ 0.10 sec., the damping constant $\varepsilon/\omega=0.5\sim0.6$.

Now, as for the anemometer, it is necessary to obtain the two horizontal components of the pressure intensity of the natural wind. Of course, the anemometer is installed at a certain position to observe the wind variation, as already discussed, of the two horizontal components. From these demands, we must use a sphere as the part of the meter against which the wind, of which the pressure intensity is to be measured, blows directly, as schematically shown in Fig. 1. Hereupon, we determined the diameter of the sphere in the following way. Taking $R_e$, $V$, $d$ and $\nu$ as Reynolds number, wind velocity, diameter of the sphere and kinematic viscosity of the air respectively, we know generally the following relation:

$$R_e=V\cdot d/\nu\,. \qquad \cdots\cdots\cdots\cdots\cdots\cdots(2)$$

Putting $R_e=3\times10^5$, $\nu=0.1456$ cm$^2$/sec, and $V=60$ m/sec, we obtain

3) The free vibration periods of wooden houses are 0.1$\sim$1.0 sec. for one-storied and three-storied house, those of Gojyu-no-Tô tower are 1.0$\sim$2.0 sec., and those of steel towers for electric transmission lines are nearly 1.0 sec.

the following value of $d$: $d=7.28$ cm. Therefore, when we take the value of $d$ as 10 cm, the total resistance of the sphere increases proportionally to the wind velocity, or the wind pressure, and for the values of the wind velocity 0~44 m/s (wind pressure 0~119 kg-wt/m$^2$), and for the case of $V=44$ m/sec, the total resistance of the sphere becomes 0.39 kg. The relation (2) shows us, moreover, that for the respective spheres of $d=15$ cm and 20 cm, the total resistances of them become proportional to the wind velocity $V=0\sim29.1$ m/sec. and $V=0\sim21.9$ m/sec. respectively, and they show equally the maximum value of 0.39 kg for the two cases, i.e. $d=15$ cm, $V=29.1$ m/sec. and $d=20$ cm, $V=21.9$ m/sec. When the diameter of the sphere is 7.28 cm, we are, of course, able to make the resistance of the sphere increase proportionally to the wind pressure or the wind velocity until the wind velocity becomes about 60 m/sec, but for the present anemometer we take two kinds of the sphere of which the diameters are 15 cm and 20 cm respectively because in the case of small velocity of the natural wind, we want to increase the sensibility of the anemometer.

As already mentioned, we adopted a machine having an inverted pendulum with the sphere on the top of it for the present anemometer, the sphere being composed of two diameters $d=15$ cm, 20 cm. We also adopted a mechanical magnifying method of recording. Therefore from technical reasons it is desirable that the maximum velocity of the wind be recorded at the length of about 20 mm or less than 20 mm on the recording paper and also the maximum deflection of the center of the sphere be about 1 mm less than 4 mm. We adopted the two-stepped magnifying mechanism with the lever system of about 66.5 multiple lever magnification.

We will use the following notations for the respective quantities shown in Fig. 1:

$y_A$=Max. deflection of the center of the sphere fixed on the top of the inverted pendulum caused by the maximum wind velocity,

$l$=Length of the flat spring which becomes the rotation axis and also gives the restitutive moment of the inverted pendulum,

$L$=Distance between the rotation axis of the flat spring of the inverted pendulum and the center of the top sphere,

$I_s$=Sectional moment of inertia of the flat spring of the pendulum,

$E$=Longitudinal modulus of elasticity of the flat spring of the pendulum,

$W_m$=Maximum wind pressure,

$C_x$=Resistance coefficient of the sphere of the pendulum,
$S$=Max. sectional area of the sphere of the pendulum.
Then, the following formula is easily obtained:

$$y_A=\frac{Ll(L-l)}{EI_s}C_xW_mS. \quad \cdots\cdots\cdots\cdots(3)$$

Using this formula, we determined the dimensions of the flat spring of the pendulum as follows. Assuming that $E=2.1\times10^{12}$ dyne/cm$^2$, $y_a=0.14$ cm, $l=3$ cm, $W_m=52.7$ kg/m$^2$, $C_x=0.42$, $S=\pi d^2/4$, $d=15$ cm, and $L=84.3$ cm, we obtained the following value of $I_s$: $I_s=6.43\times10^2$ cm$^4$. Therefore, when the two flat springs of breadth of 2.5 cm are used, the respective values of thickness of the two springs become 2.04 mm. Of course, in order to obtain the expression $y_A$, it was assumed that the upper part of the pendulum stem above the flat spring does not show any deformation due to the wind pressure applied on the sphere fixed to the top of the pendulum stem. To satisfy this assumption, as shown in Fig. 1, the structure of the stem becomes as follows: The lower part of the stem is an aluminium pipe having the length of 570 mm and the outer and inner diameters of 50 mm & 44 mm, and the upper part of it becomes also an aluminium rod of the length of 200 mm and the diameter of 23 mm. The lower part of the rod and upper part of the pipe are fixed to each other by screwing, and therefore the transversal vibration period of these combined stem becomes very short as about 0.007 sec., which is the calculated value.

Now, as the magnifying method for the present anemometer, we adopted the mechanical one which is quite of the same mechanism as the acceleration-seismometer[1] designed by the late Prof. Ishimoto. As shown in Fig. 1, the present magnifying mechanism is of the two-stepped lever system and the levers have the characters shown in Table 1.

Table I.

| Lever \ Arms | Length of short arm | Length of long arm | Moment of inertia |
|---|---|---|---|
| The first-step magnifying lever | $l_1=15$ mm | $L_1=150$ mm | $I_1=250$ gr cm$^2$ |
| The second-step magnifying lever | $l_2=15$ mm | $L_2=100$ mm | $I_2=10$ gr cm$^2$ |

The distance $L_3$ between the rotation axis of the inverted pendulum

4) M. ISHIMOTO, *Bull. Earthq. Res. Inst.*, **9** (1931).

and the first-step magnifying lever is taken as 9.0 cm for the present case. The equation of motion of the present anemometer due to wind pressure $W$ is expressed by

$$\left(I_0+I_1\frac{L_0^2}{l_1^2}+I_2\frac{L_0^2L_1^2}{l_1^2l_2^2}\right)\frac{d^2\theta}{dt}+\lambda\frac{d\theta}{dt}+K_0\theta=Wh\,. \quad \cdots\cdots(4)$$

From this equation, we can see that the moments of inertia $I_0$, $I_1$, $I_2$, especially those of the first-step and the second-step magnifying levers $I_1$ and $I_2$ should be as small as possible, because they have the tendency to prolong the natural period[5] of the anemometer. The moment of inertia of the spherical head on the top of the pendulum stem has of course the large effect to increase the moment of inertia $I_0$, and therefore for minimizing it the spherical head used for the present machine is of copper-made thin shell. The details of the construction of it is explained in page 325 of this paper. Therefore, the moment of inertia of the pendulum body $I_0$ is taken as 13,000 gr cm$^2$, and the respective values of $I_1$ and $I_2$ are shown in Table I. The sectional form of the first-step lever of aluminium is of the cross type and the long arm of the second-step lever is a straw pipe of about 2 or 3 mm diameters. Therefore, the increase of the moment of inertia of the anemometer due to both the mechanical magnifying mechanism and the mechanical recording system becomes only about 2% for both two spheres which are fitted to the top of the stem of the inverted pendulum.

We adopted for the anemometer an air damper with an aluminium piston of 10 cm in outer diameter and an aluminium cylinder of 10.02 cm inner diameter. The clearance[6] between the piston and the cylinder

---

5) Natural period $T=2\pi\sqrt{\frac{I}{K_0}}$, where $I=I_0+I_1\frac{L_0^2}{l_1^2}+I_2\frac{L_0^2L_1^2}{l_1l_2}$.

6) The clearance $e$ becomes as follows:

$$e=\left(\frac{6\pi\eta l}{\lambda}\right)^{1/3}\cdot rL\,, \quad \text{where}$$

$r$=Outer radius of the piston of the air damper,
$l$=Height of the same piston,
$L$=Distance between the rotation axis of the inverted pendulum of the anemometer and the piston axis of the air damper,

$\lambda=2\varepsilon I=2\omega I=\frac{4\pi I_0}{T_0}$ where $\varepsilon/\omega=1$,

$T_0$=Natural period of the inverted pendulum of the anemometer,
$I_0$=Moment of inertia of the inverted pendulum of the anemometer,
$\eta$=Coefficient of viscosity of air.

For the present anemometer, taking $r=5$ cm, $L=18$ cm, $l=5$ cm, $T_0=0.1$ sec, $I_0=4\times10^6$ gr-cm$^2$. and $\eta=1.81\times10^{-4}$ in C. G. S. Unit, we obtained $e=0.01$ cm.

inner wall becomes, therefore, 0.01 cm. The precision adjustment of the damping degree of the air damper is made by handling the cock attached to the damper to secure suitable entrance and exit of air through the cock.

By using the design of the anemometer discussed in the preceding section, we obtained the two new-designed anemometers which are shown in Figs. 2a, 2b & 2c. As shown in Figs. 2a, 2b and 2c, the actual anemometer is constructed so as to obtain the two components of the horizontal wind pressure, and therefore the springs used for the rotation axes of the inverted pendulum are composed of two sets and one of them is connected to the base plate of the anemometer and the other to the lower end of the pendulum stem, and each set has two flat springs. Of course, these two sets of spring are fixed to form a right angle with each other. Each set of spring is composed of two flat spring plates which give the restitutive force to the inverted pendulum of the anemometer. Therefore these two sets of spring give respectively the restitutive forces whose direction of action is perpendicular to each other. Two air-dampers are used, as shown in Figs. 2b and 2c, of which the one cylinder is fixed to the base of the anemometer, and the other cylinder is fixed to the stem of the inverted pendulum and can move freely in two horizontal components of direction.

The recording system of the present anemometer is a kind of mechanical one, and is composed of smoked paper system which is commonly used in the field of seismometer in Japan. The driving motor of the recording drum for the present recording apparatus is a synchronous motor of 6 watt and 1 r.p.m.

By the gear mechanism, the peripheral speeds of the recording smoked paper on the drum are made to have three kinds such as 0.4 cm/sec, 0.1 cm/sec and 0.04 cm/sec. The drum is made of aluminium, as in the case of the Ishimoto acceleration-seismometer[7].

As may be seen in Fig. 2a, all the parts except the spherical part blown directly by wind of the present anemometer are set in a suitable cover for the purpose of avoiding the attack of the wind pressure. The lower part of the cover is a cylinder, which forms the foundation of the anemometer. Both the top and bottom thick plates of it is made of casting, and the top thick plate becomes the base plate for the inverted pendulum of the anemometer. Of course, to this base plate is fixed one of the two sets of the flat springs giving the restitutive

7) M. ISHIMOTO, *loc. cit.*

forces to the pendulum. The recording drum is set on the bottom plate of this cylinder foundation, and the diameter and the height of this cylinder become 80 cm and 50 cm respectively, and the top and bottom plates are made of cast iron and the cylinder wall is composed of common steel plate. The total height of the anemometer becomes 200 cm, and it is made heavy, the weight being 100 kg-wt, so as to avoid the rattling and shaking motions of the base and the cover of the anemometer when attacked by a strong wind.

### 3. The character test of the anemometer.

The records of the wind pressure are taken by the smoked paper method as already explained. Therefore solid friction between the recording needle and the smoked paper affects badly the sensitivity of the anemometer. This needle is pivoted to the end of the straw pipe which becomes the long arm of the second-step magnification. We first studied this solid friction by a common method as follows:

The solid friction term $\rho$ and the damping ratio $V$ are connected by $V=\{W_k-2\rho(1+V)\}/W_{k+1}$, where $W_k$, $W_{k+1}$ are respectively the $K$th and $(K+1)$th double amplitudes recorded on the smoked paper in the state of free damped vibration of the anemometer. Therefore, plotting $W_k$ and $W_{k+1}$ on the section papers as shown in Fig. 3, we obtained, using the above expression and Fig. 3, the following values of $V$ and $\rho$:

$V=1.05$, $\rho=0.025$ mm.

Therefore the solid friction $\rho'$ becomes as follows:

$\rho'=1.86\ \mathrm{kg/m^2}\times 0.025\ \mathrm{mm}$

$=0.46\ \mathrm{kg/cm^2}$.

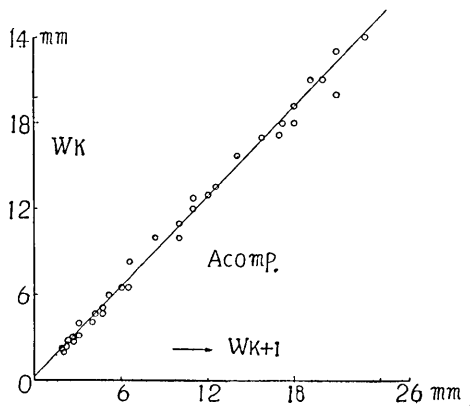


Fig. 3.

From this experiment, we can see that the present anemometer with smoked paper recording mechanical method cannot record wind pressure less than 0.46 kg/cm², or in other words, it can record wind velocity greater than 0.9 m/sec.

Now, due to its construction, the present anemometer has some effective inertia. Therefore, when its foundation is vibrated through

some source, it comes to have the tendency of doing the action of a vibrograph. Of course, the effective masses of the inverted pendulum are made as small as possible, but the unavoidable fact is that the moment inertia of the apparatus does its action as a vibrograph which is caused by a vibration source applied to the base of the foundation of the machine. Hereupon, using a rotary with an unbalanced mass of small scale, we applied a horizontal force to the anemometer to obtain the sensibility as a vibrograph, and in addition to this experiment we installed a acceleration seismograph[8] on the top face-plate of the base cylinder, for comparing both of these experimental results. The experimental results are shown in Figs. 4a and 4b, in which the abscissae show the varied period of the applied unbalanced forces and the ordinates the deflection $a_1$ of the anemometer in Fig. 2a and the deflection $a_2$ of the acceleration seismograph. Moreover, Figs. 4a and 4b show the respective results referring to the two components A and B. These figures show that the present anemometer has somewhat the properties

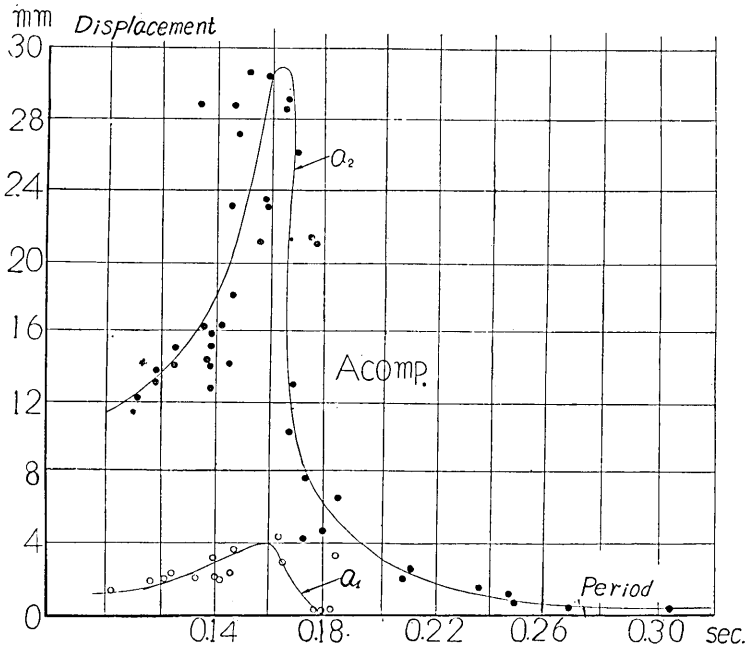


Fig. 4a. A comp.

8) Portable acceleration seismograph of period 0.1 sec, sensibility = 2.0 gal per mm on the record and critical damping.

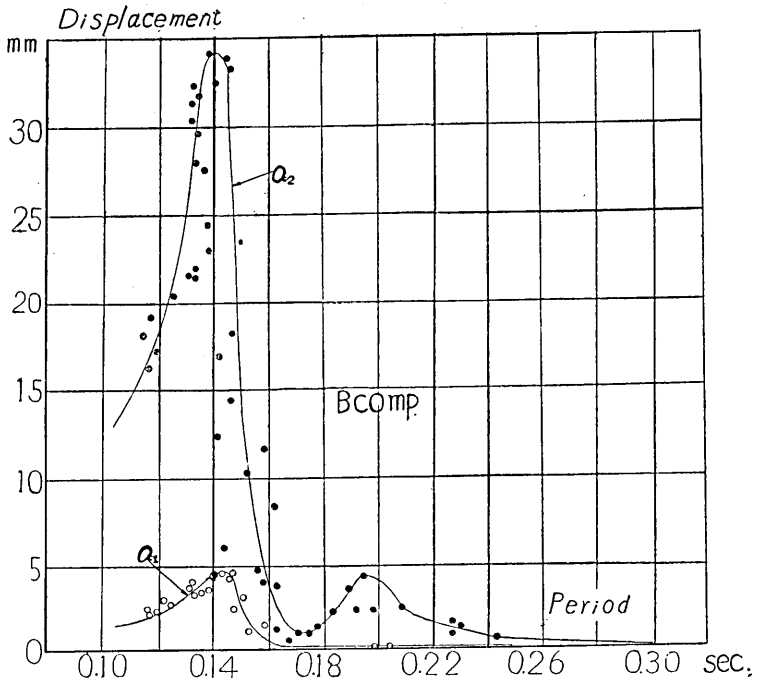


Fig. 4b. B comp.

of a vibrograph, but the ratio of two deflections $a_1/a_2$ assumes, as shown in Fig. 5, the constant value 1/8 for applied periodic force of which the period becomes greater than 0.12 sec. Therefore, we can correct the recorded deflections of the anemometer by installing an acceleration seismograph in the base cylinder of the anemometer.

Next, as a sensibility test of the present anemometer the following experiment was carried out. Applying the periodic force horizontally on the center of the spherical head of the present machine,

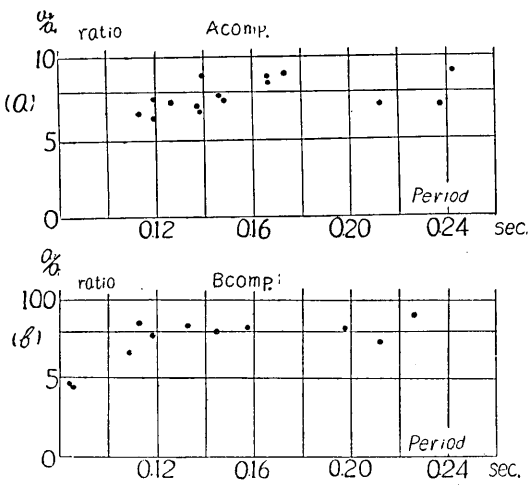


Fig. 5. A comp. B comp.

we observed the deflection of it, which is shown in Fig. 6. From Fig. 6, we can see that the period of the present machine, when it has a spherical head of 20 cm diameter, becomes somewhat longer than that designed, and it becomes about 0.075 sec. for the two horizontal components (A, B) equally, and therefore the present machine has a constant sensibility for the periodic pressure whose period becomes longer than 0.20 sec. For the case of 15 cm diameter spherical head, we obtained the same properties of sensibility, and the natural periods for the two horizontal components become of course shorter than those in the case of 20 cm diameter spherical head, i.e., 0.070 sec.

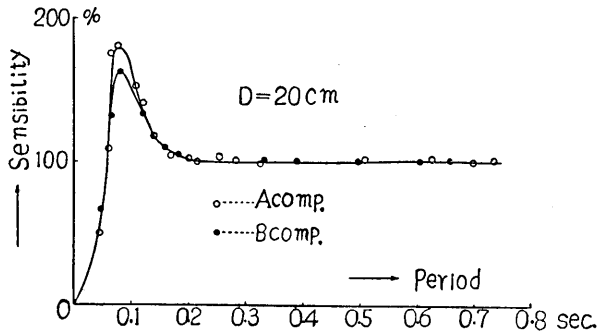


Fig. 6.

The results of the wind tunnel test[9] of the present anemometer are shown in Fig. 7 in which the abscissa corresponds to wind pressure in kg-wt/m² and the ordinate to the reading of the displacement in mm on the recording paper of the machine for the respective cases of 20 cm-, 15 cm-diameter spherical heads. From this figure, we can see that the proportionality is ascertained for the present machine, and the sensibilities are 28.0 kg-wt/m² for 20 cm-diameter spherical head and also 45.5 kg-wt/m² for 15 cm-diameter one. The statical test of the present machine was also carried out, in which the statical loads are horizontally applied to the center of the spherical head.

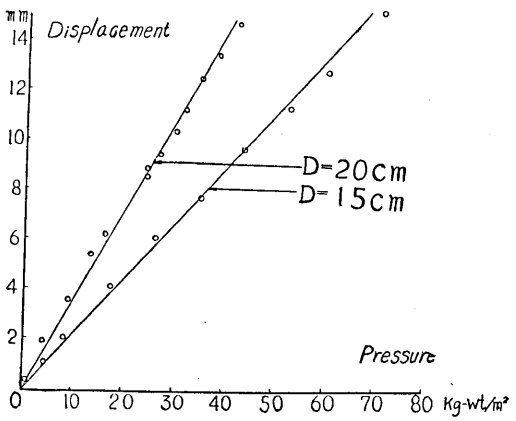


Fig. 7. Wind tunnel test.

9) The test was carried out with 1.5 m–3.0 m section wind tunnel belonging to the former Aeronautical Research Inst., University of Tokyo.

The results of the statical test are shown in Fig. 8 in which the statical loads in gram applied are taken in abscissa, and the deflection $\delta$ in mm of the recording needle in ordinate. In this figure, we can see that the deflection $\delta=1.0$ cm corresponds to the total resistance 435 gr for the 20 cm diameter spherical head and 443 gr for the 15 cm diameter one respectively. Therefore, using the relation $R=C_x q \cdot S$, where $R$=total resistance, $q$=pressure in unit area, and $S$=diametral area of section, we calculated the value of the resistance coef. $C_x$ as follows;

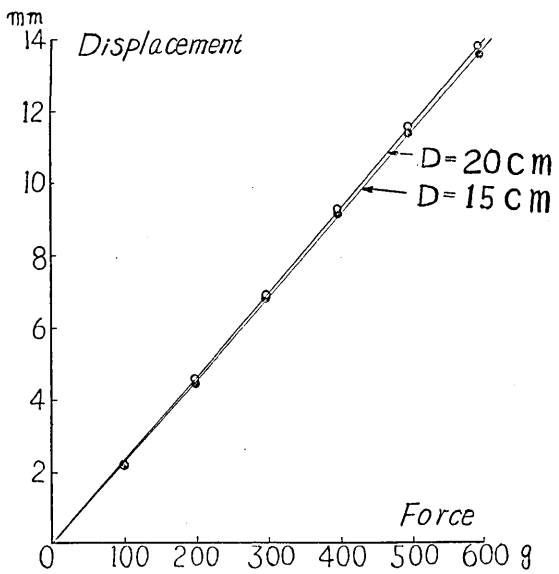

Fig. 8. Statical test.

$C_x=0.48$ for 20 cm dia. spherical head,
and $C_x=0.53$ for 15 cm dia. spherical head.

The value of this resistance coefficient for 15 cm diameter spherical head becomes larger than that for 20 cm dia. spherical head about 5%. This fact, we think, may be explained as follows: The aluminium bowl fixed to the top of the stem of the inverted pendulum of the machine, the position of which is under the spherical head as may be seen in Fig. 2a, 2b, for the purpose of protecting the interior of the machine against rain, affects unfavourably the wind resistance. Namely the effect of this bowl, of which the effective section area is 7 cm, on the resistance for the case of 15 cm diameter head becomes more serious than for the case of 20 cm diameter head.

The spherical heads used for the present machine are of copper-made thin shell, and the two spherical bowls are made from copper plate of 0.5 mm thickness by the operation of the spatula drawing method, and are soldered at the diametral circle. A stem of steel rod of 10 mm diameter is set through the interior of the sphere, one end of it is soldered to the interior top of the sphere, and the other end, which is outside the sphere, is fixed to the top of the stem of the inverted pendulum by screw.

## 4. Observation and analysis of the natural wind by the present anemometer.

The present anemometer was installed on the floor of a wooden-made framework constructed on the roof of a Japanese ware-house at Inatori-machi, Izu Peninsula, Shizuoka Prefecture. The location of the installation of the machine and the environment of the location are roughly shown in the topographic map of Fig. 9. The east side of the location faces Pacific Ocean, and both the north and west sides face the Izu mountain range. Fig. 10 is the photograph of the anemometer installed on the roof of the ware-house at the location explained above.

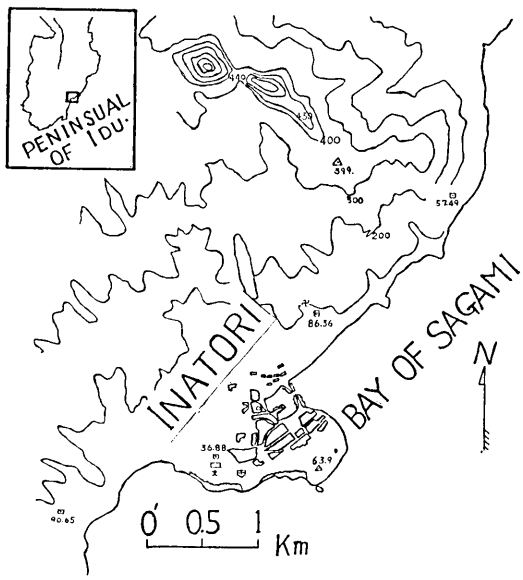


Fig. 9.

Now, some of the records of natural winds obtained by the present anemometer are shown in Figs. 11a, 11b. They are so complicated that it is very difficult to study the structure or the breath of the natural winds. Thus, it is also difficult to obtain the so-called breaths of natural wind or the periods of variation of the wind pressure or wind velocity.

By the following method, we analysed the records in order to obtain the period of the natural wind. The records used for the present analysis are those of the monsoons of the South-West wind of December 2, 1940, as well as those of the North-East wind of March 2, 1941, both having their own peculiar characters.

By investigating these records minutely, we found that during the period between two zero wind pressures there are complicated undulations of wind pressure, and also many maximum and minimum pressure intensities, and that the wind having the greatest intensity may be expected during this period. Therefore, it may be reasonable to assume that the variation of the wind pressure are generally expressed by the

diagrammatic schema shown in Fig. 12.

Considering the upper schema shown in Fig. 12, we shall assume $T_0$ to be the period of zero wind pressure. $T_0$ in this case is the duration time from the 1st zero wind pressure to the next zero wind pressure. We will also assume the largest wind pressure in this period $T_0$ to be $Q_0$.

As may be seen in the lower schema shown in Fig. 12, the wind pressures have a complicated undulation character with many maximum and minimum values of pressures for the duration time $T_0$. Putting the duration time between the two continued minimum points as $t_1$, we will assume $t_1$ to be the period of the 1st order. (see $t_1$ of Fig. 12.)

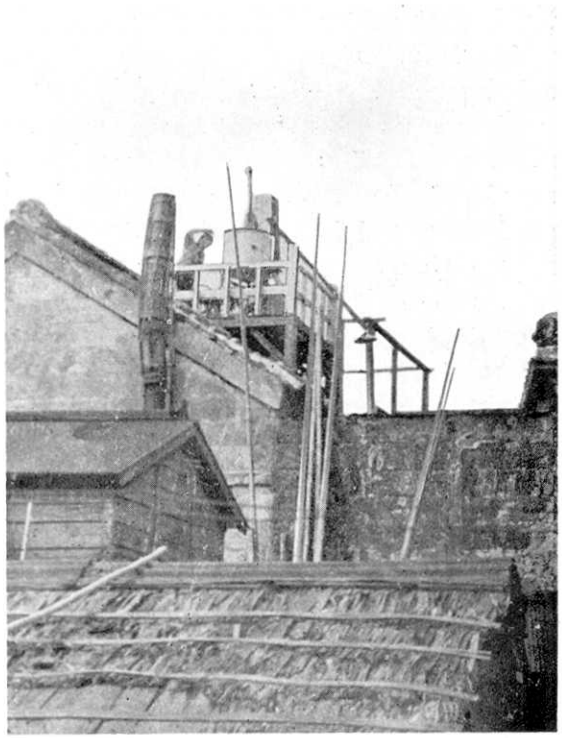

Fig. 10. Anemometer installed on the roof of a ware-house.

We assume that the respective two differences between both two extreme ends of the time $t_1$, or two continued minima and the maxima in time $t_1$ are shown by $q_i$ and $q_{i+1}$.

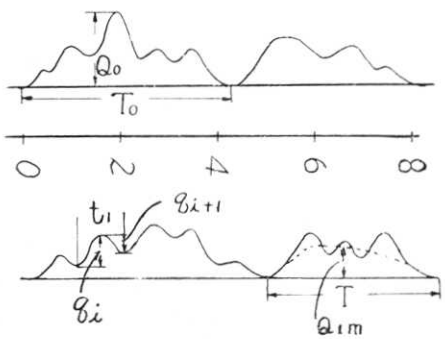


Fig. 12.

Then putting the arithmetic mean of $q_i$ and $q_{i+1}$ as $q_1$ or $q_1=(q_i+q_{i+1})/2$, we will assume $q_1$ to be the maximum wind pressure with period $t_1$.

The mean valued curves connecting the mean values of the maxima and minima which occur between the time $T_0$, shall be taken as the mean wind pressures of the 1st order. We will also express

the largest values of them for the duration time $T_0$ by the letter $Q_1$ which is taken as the largest mean valued wind pressure of the 1st order.

For cases where we can find the maxima and minima in these mean-valued wind pressures of the 1st order, by the same method as mentioned above, we can obtain the duration time $t_2$ of continued two maxima or minima, and this duration time $t_2$ shall be called the 2nd order period.

As in the cases of obtaining $q_1$ and $Q_1$, the largest wind pressure $q_2$ corresponding to the period $t_2$, and the largest mean-valued wind pressure of the 2nd order $Q_2$ are also generally obtainable.

By the same treatment as explained above, the 3rd order quantities $t_3$, $q_3$, $Q_3$, and the 4th order quantities $t_4$, $q_4$, $Q_4$, etc. are also obtainable. In brief, by using these obtained quantities such as $T_0$, $Q_0$ and $t_1$, $q_1$, $Q_1$, $t_2$, $q_2$, $Q_2$, ...., $t_n$, $q_n$, $Q_n$, we intend to conduct analysis of the natural wind structures for the following three cases; (1) breath of natural wind, (2) wind pressure and breath, and (3) wind pressure and the blowing direction.

## 5. Analysis results I. Breath or period of natural wind.

From the records of the wind pressure obtained by the present anemometer on Dec. 2 in 1940 and March 2 in 1941, we read first the values of $T_0$ and $t_1$ which are already respectively defined in the preceding section.

Then, grouping the values of $T_0$ and $t_1$ by the following method, we will study the statistical natures of them respectively.

For example, express the two values of $T_0$ by $T_{0i}$ and $T_{0i}'$ respectively. Then, all the values of $T_0$ between $T_{0i}$ and $T_{0i}'$ are represented by the mean value of $T_{0i}$ and $T_{0i}'$ or $T_{0m}$ in case $T_{0m}=(T_{0i}+T_{0i}')/2$, when they are satisfied by the following expression:

$$2(T_{0i}-T_{0i}')/(T_{0i}'+T_{0i})=1/10 \quad \text{.....(10)}$$

Now we assume that the total sum $n$ of all the values of $T_0$ between $T_{0i}$ and $T_{0i}'$ under the condition expressed by (10) shows the fluctuation degree of $T_0$. By this conception, we obtained the frequency curve of $T_0$ or $T_0 \sim n$ curve which is necessary for studying the statistical natures of the variation of the breath of the natural wind.

Figs. 13 and 14 show $T_0 \sim n$ curves for the 10 minutes observation for the two cases, i.e., the SW wind from 14 h 5 m to 14 h 15 m on Dec.

2, 1940 and NE wind from 16 h 21 m to 16 h 31 m on March 2, 1941. From these figures, we can see that for the SW wind, $T_0$ whose values are 1.7 sec., 3.2 sec., 6.1 sec. and 15 sec., become predominant and for the NE wind $T_0$ whose values are 0.5 sec. and 1.6 sec. become predominant.

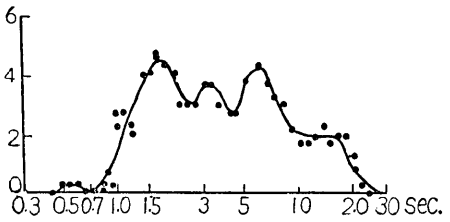


Fig. 13. Statistics of $T_0$ period of SW wind from 14 h 5 m to 14 h 15 m, Dec. 2, 1940.

Next, taking the record of SW wind from 14 h 14 m to 14 h 15 m 20 s on Dec. 2, 1940 and that of NE wind from 16 h 21 m to 16 h 23 m on March 2, 1941 by the same procedures as in the preceding cases of $T_0$, we obtained $t_1 \sim n$ curves as shown in Figs. 15 and 16 in which $t_1$ becomes the period of the 1st order explained in the preceding section. From these figures, we can see that for SW wind, $t_1$ with value of 0.6 sec. and 0.95 sec. become predominant and for NE wind, $t_1$ with value of 0.5 sec. becomes predominant.

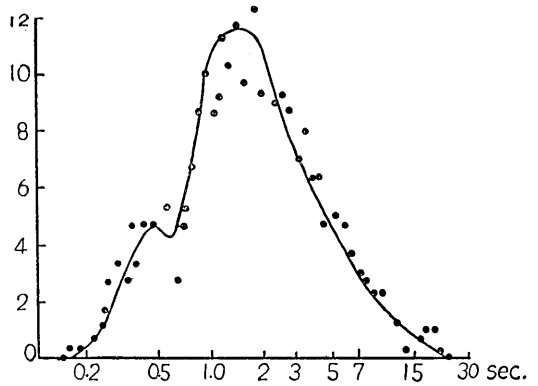


Fig. 14. Statistics of $T_0$ period of NE wind from 16 h 21 m to 16 h 31 m, March 2, 1941.

From these four figures (Figs. 13, 14, 15 and 16), we can see generally that for two cases of breath such as $T_0$ and $t_1$, those corresponding to the SW wind become somewhat longer than those corre-

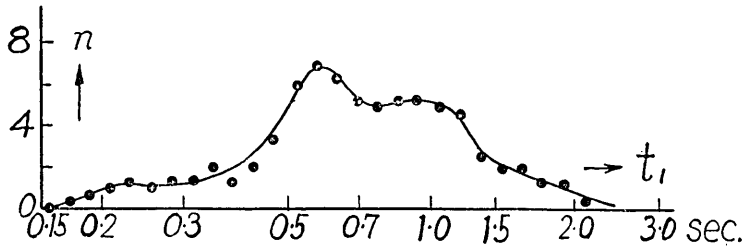


Fig. 15. Frequency curve of $t_1$ for the SW wind from 14 h 14 m to 14 h 15 m 20 s, Dec. 2, 1940.

sponding to the NE wind.

Now we can see that the SW wind is the one passing over the mountain district of a generally complicated topography and the NE wind is the one passing wholly over the sea surface which is comparatively simple. From these two facts, we can say, about the properties

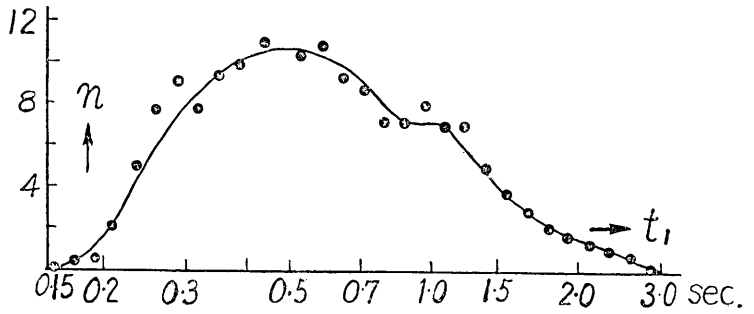


Fig. 16. Frequency curve of $t_1$ for the NE wind from 16 h 21 m to 16 h 23 m, March 2, 1941.

of natural wind breath whose periods differ according to the blowing directions, that there is some correlation between the breath periods of natural winds and the degree of the complication of the topography over which the wind blows.

## 6. Analysis results II. Periods and pressures of natural blowing winds.

With the same records used in obtaining the $T_0 \sim n$ curves in the preceding section, we will study the properties of $T_0 \sim Q_0$, $T_1 \sim Q_1$, $t_1 \sim q_1$ curves in this section. Of course, the respective measurings of $Q_0$, $T_1$, $Q_1$, $t_1$ and $q_1$ have been already defined in the preceding section.

Concerning the SW wind of the three cases, i.e., from 14 h 14 m to 14 h 15 m on Dec. 2, 1940, from 13 h 49 m to 13 h 59 m on Dec. 2, 1940 and from 14 h 5 m to 14 h 15 m on Dec. 2, 1940, we obtained (a) in Figs. 17a and (a), (b) in Fig. 17b in which the relation between $T_0$ and $Q_0$ for the respective three cases are shown. In these figures the abscissae and the ordinates show respectively the $T_0$ in sec. in log. scale and $Q_0$ in kg-wt/m$^2$.

Next, concerning the NE winds of the three cases, i.e., from 16 h 21 m to 16 h 22 m on March 2, 1941, from 16 h 21 m to 16 h 31 m on

March 2, 1941, from 17 h 45 m to 17 h 55 m on March 2, 1941, and from 16 h 22 m to 16 h 23 m on March 2, 1941, we obtained (a) in Fig. 18a, (a), (b) in Fig. 18b and (a) in Fig. 18a, in which the relations of $T_0$ and $Q_0$ of these four cases are shown respectively. The units of both abscissae and ordinates in these figures, are the same as in the figures for SW winds. From these figures for both the SW and the NE winds, we can see that the breaths of period $T_0$ having the effective maximum pressure become as shown in Table II.

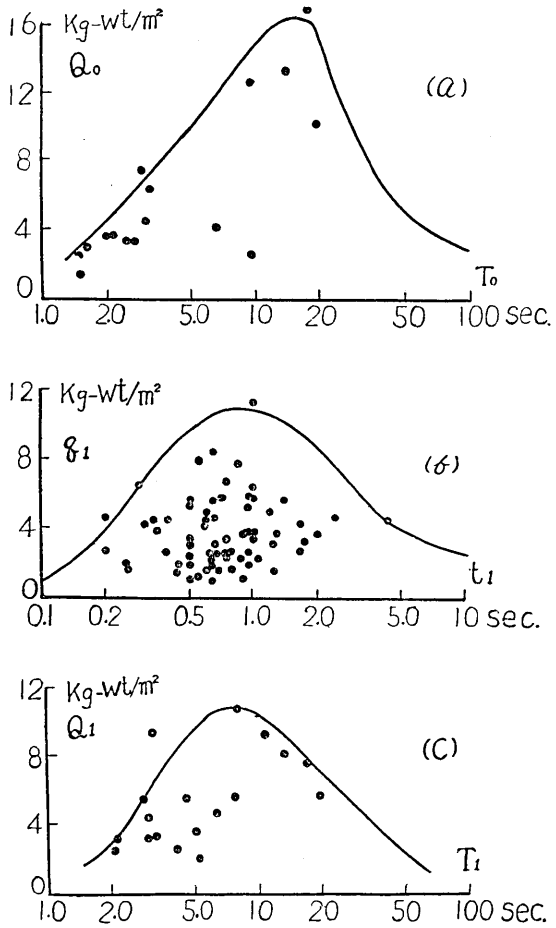


Fig. 17a. The SW wind of 14 h 14 m~14 h 15 m, Dec. 2, 1940.
(a): $T_0 \sim Q_0$, (b): $t_1 \sim q_1$, and (c): $T_1 \sim Q_1$.

Table II shows that in spite of the difference of the observation time, both the NE wind and the SW wind have respectively the maximum wind pressures $Q_0$ for a suitable breath of period $T_0$. For example, they ($Q_0$) become maximum respectively when breath $T_0$ becomes 5 or 9 sec. for the NE wind, and when $T_0$ becomes 15 or 17 sec. for the SW wind. Moreover, it is a remarkable fact, that the breath $T_0$ giving effectively maximum wind pressure becomes different in accordance with the blowing direction and the breath $T_0$ corresponding to the SW wind becomes two or three times longer than that of the NE wind.

By the same treatment as that which made clear the relation between $T_0$ and $Q_0$, we obtained the relations between $t_1$ and $q_1$ and also those between $T_1$ and $Q_1$, which are respectively shown in (b) and (c)

Table II. Breath period $T_0$ of maximum pressure $Q_0$.

| Wind | $T_0$ giving max. pressure | Observation date |
|---|---|---|
| NE wind | 5 sec., 9 sec. | 16 h 21 m~16 h 22 m, 16 h 21 m~16 h 31 m, 17 h 45 m~17 h 55 m, 16 h 22 m~16 h 23 m } March 2, 1941. |
| SW wind | 15 sec., 17 sec. | 14 h 14 m~14 h 15 m, 13 h 49 m~13 h 59 m, 14 h 5 m~14 h 15 m } Dec. 2, 1940. |

in Fig. 17a, in (b) and (c), in Fig. 18a, and also in (b) and (c) in Fig. 18c. The measurings of $t_1$, $q_1$, $T_1$, and $Q_1$ in these Figs. have already been defined in the preceding section. These figures show that the wind pressures defined by $q_1$ and $Q_1$ have also the maximum values corresponding to suitable breaths of period $t_1$ and $T_1$ respectively in spite of the difference of the blowing direction of the wind, and the values of $t_1$ and $T_1$ giving maximum values as shown in Table III.

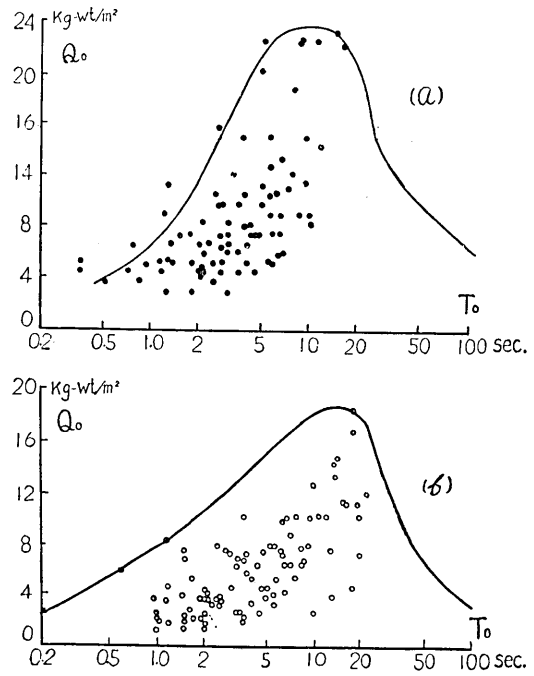


Fig. 17b. (a): $T_0$~$Q_0$ for the SW wind of 13 h 49 m~13 h 59 m, Dec. 2, 1940.
(b): $T_0$~$Q_0$ for the SW wind of 14 h 5 m~14 h 15 m, Dec. 2, 1940.

From Table III, we can see that, as in the case of $T_0$ and $Q_0$ shown in Table II, in spite of the blowing direction of natural wind, there are wind breath periods $T_1$ and $t_1$ which give respectively maximum wind pressure defined by $Q_1$ and $q_1$ respectively. It is also remarkable that the breath periods $t_1$, $T_1$ of the SW wind becomes two times longer than those of the NE wind. Now, for the respective winds of NE and SW under discussion in the above paragraph, we obtained Table IV, in which the

Table III. The breath periods $t_1$, $T_1$ giving the maximum values of $q_1$ and $Q_1$ wind pressure distribution.

| Wind direction | $t_1$ giving max. values of $q_1$ | $T_1$ giving max. values of $Q_1$ | Observation date |
|---|---|---|---|
| NE wind | 0.4–1.0 sec. | 4 sec. | 16 h 21 m~16 h 22 m, March 2, 1941 |
| SW wind | 0.9 sec. | 8 sec. | 14 h 14 m~14 h 15 m, Dec. 2, 1940 |

maximum values of wind pressure of $q_1$ and $Q_1$, and also their ratio $q_1/Q_1$ are given in addition to the values of $t_1/T_1$, in which $t_1$ & $T_1$ are given in Table III.

Comparing the SW wind and the NE wind, we understand that they have respectively some interesting characters, as may be seen in Table IV. For SW wind, in the breath period $T_1$ such as 8 sec. of pressure intensity $Q_1$=11 kg-wt/m², there is a breath period $t_1$ of about 1/10 times of $T_1$, but their pressure intensity $q_1$ becomes 11 kg-wt/m² which is equal to $Q_1$. For the NE wind, in the breath period $T_1$ such as 4 sec., there is a breath period $t_1$ of about 1/10~1/4 times of $T_1$ of which the max. pressure intensity $q_1$ becomes about 60% of $Q_1$.

This analysis shows that the structure of the SW natural wind becomes more complicated than that of the NE natural wind, which fact is clear when we compare the two records of both winds. (See Figs. 11a, b.) And this property, we think, may perhaps be explained from the

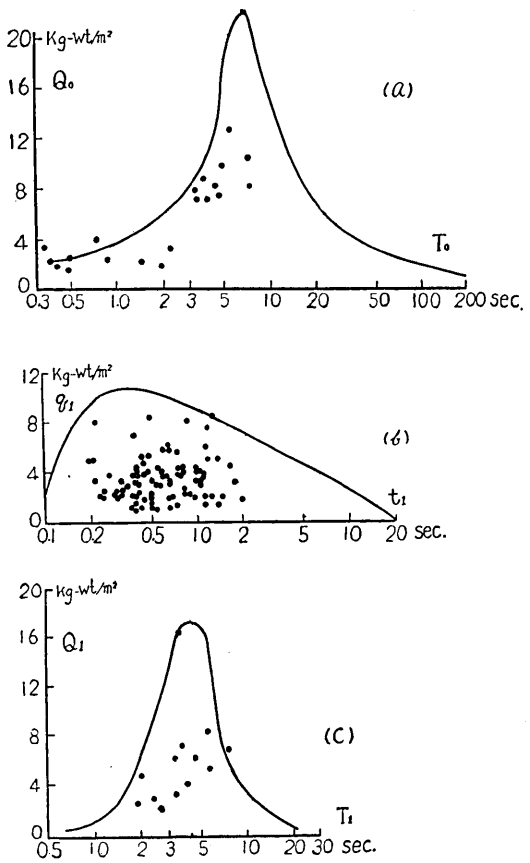


Fig. 18a. NE wind, 16 h 21 m~16 h 22 m, March 2, 1941.
(a) $T_0$~$Q_0$, (b) $t_1$~$q_1$, (c) $T_1$~$Q_1$.

Table IV. Max. values of $q_1$ and $Q_1$.

| Kind | Max. wind pressure | | | Ratio of Periods of breath $t_1/T_1$ |
|---|---|---|---|---|
| | $q_1$ in kg-wt/m² | $Q_1$ in kg-wt/m² | Ratio $q_1/Q_1$ | |
| NE wind | 10.5 | 17.0 | 0.62 | 0.10 |
| SW wind | 11.0 | 11.0 | 1.0 | 0.11 |

(Remark: $t_1$ and $T_1$ are given in Table III.)

effect of the topography of the districts over which the natural wind blows, as already discussed in the preceding section.

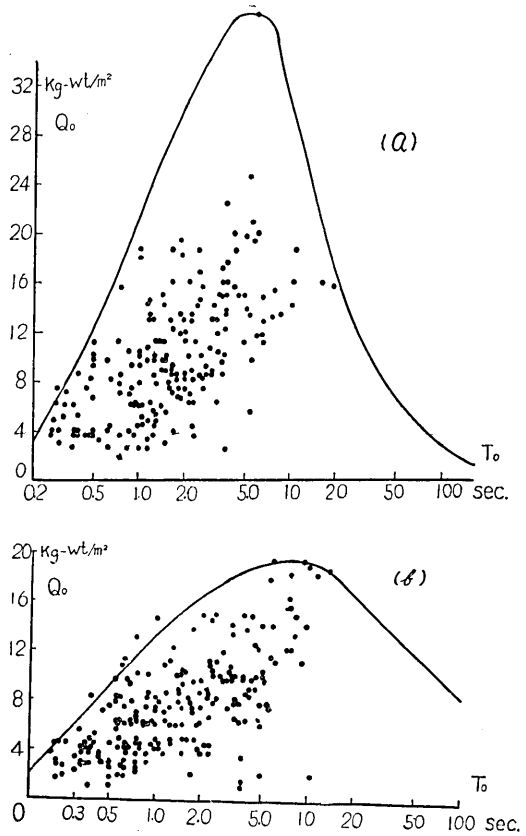


Fig. 18b. $T_0 \sim Q_0$ curves for NE wind.
(a) 16 h 21 m~16 h 31 m, March 2, 1941.
(b) 17 h 45 m~17 h 55 m, March 2, 1941.

## 7. Analysis results III. Wind pressures and wind directions.

For the purpose of studying the relation between the wind pressure and the wind direction, using the rectangular coordinates (x-, y-axis), we obtained (a), (b), (c) and (d) in Fig. 19, for the SW wind on Dec. 2, 1940, in which the plotted points correspond to every two components of wind pressures for each 5 sec. Of course these two components were obtained by the present anemometer, and the x-axis becomes the NE-O-SW component of the present position of the anemometer and the y-axis the NW-O-SW component. The four graphs (a), (b), (c) and (d) in Fig. 19 correspond to the duration time of 1 minute from 13 h 52 m to 13 h 53 m, from 13 h 57 m to 13 h 58 m, from 14 h 0 m to 14 h 1 m and from 14 h 14 m to 14 h 15 m on Dec.

2, 1940 respectively. By the same way as in Fig. 19, concerning the NE wind on March 2, 1941, we obtained five graphs as shown in Figs. 20 (a), (b), (c), (d) and (e). In these graphs, the plotted points correspond to every two components of wind pressure for every 0.25 sec.

By using the wind pressure records of the two components $p_x$ and $p_y$ of the natural wind, we could obtain the resultant pressure $p$, while its blowing direction $\varphi$ may be obtained by using the following relations:

$$\left.\begin{aligned} p^2&=(p_x)^2+(p_y)^2\,,\\ \varphi&=\tan^{-1}(p_y/p_x)\,. \end{aligned}\right\} \quad .. \quad (11)$$

By this method, we are able to study the variations of $p$ and $\varphi$ with time variation.

From Figs. 19 and 20, we can see that both the SW- and the NE-winds have the same nature, i.e., all the points showing the wind

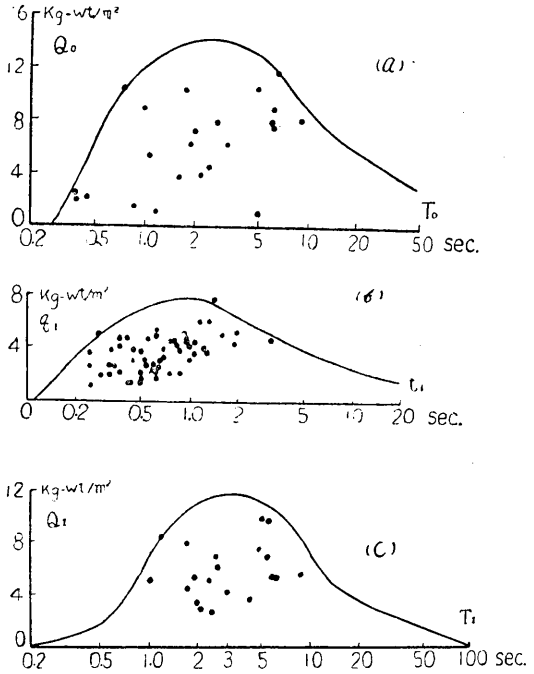


Fig. 18c. SW wind, 16 h 22 m~16 h 23 m, March 2, 1941.
(a) $T_0$~$Q_0$, (b) $t_1$~$q_1$, (c) $T_1$~$Q_1$.

Table V.

| Wind | Observation date | Max. wind pressure $p$ (in kg-wt/m²) | Direction $\varphi$ (in degree) |
|---|---|---|---|
| SW-wind | $13^h52^m$~$13^h53^m$ | 12.8 | 36 |
| | 13 57 ~13 58 | 13.8 | −61 |
| | 14 0 ~14 1 | 16.9 | 57 |
| | 14 14 ~14 15 $20^s$ | 16.5 | 16 |
| NE-wind | $15^h18^m$~$15^h19^m$ | 19.0 | 191 |
| | 16 21 ~16 22 | 39.7 | 174 |
| | 16 22 ~16 23 | 18.9 | 169 |
| | 16 31 ~16 32 | 26.1 | 188 |
| | 17 41 ~17 42 | 18.5 | 180 |

pressure for a certain time interval are included in an ellipse of which the long axis becomes the maximum wind pressure for that time interval.

Table V shows the maximum pressure $p$ and its direction $\varphi$ which are expressed by (11) for respective one minute durations shown in Fig. 19 (a), (b), (c), (d) and Fig. 20 (a), (b), (c), (e) and (d) which correspond respectively to the SW-winds and the NE-winds.

As may be seen from Figs. 19 & 20 and also Table V, for these time duration for the present case, the blowing directions of these

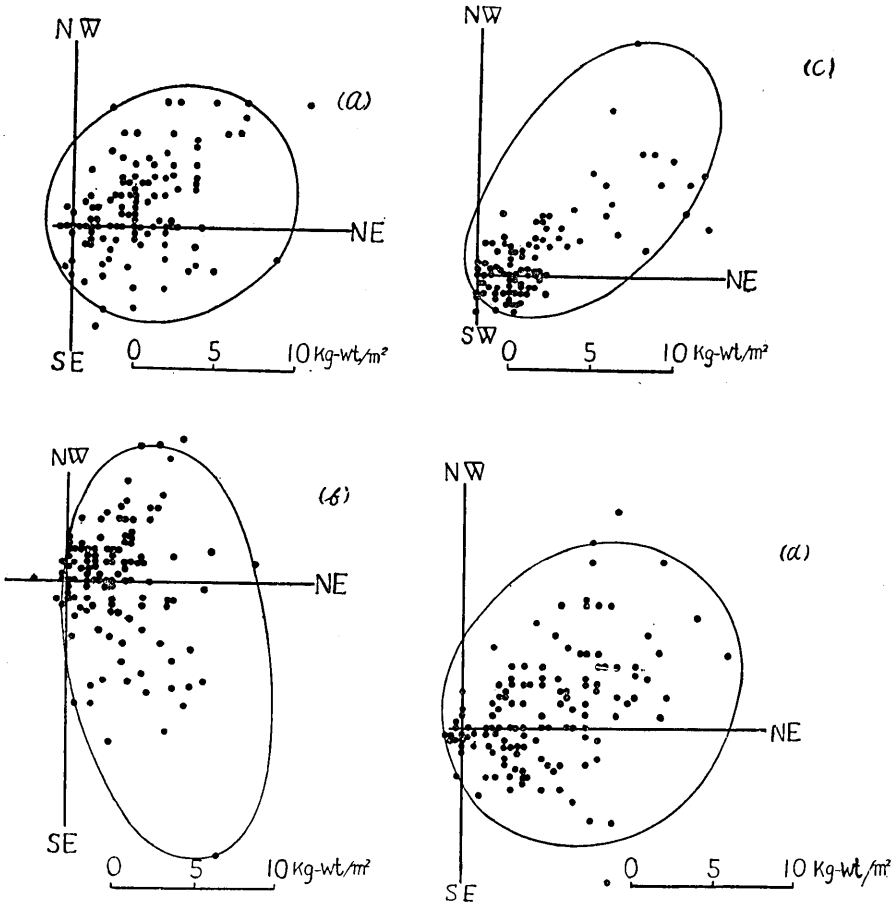


Fig. 19. Relation between wind pressure and wind direction for the SW wind.
(a) 13 h 52 m~13 h 53 m, Dec. 2, 1940,
(b) 13 h 57 m~13 h 58 m, Dec. 2, 1940,
(c) 14 h 0 m~14 h 1 m, Dec. 2, 1940,
(d) 14 h 14 m~14 h 15 m 20 s, Dec. 2, 1940.

maximum pressure for the SW wind vary distinctly for wide range such as 118° from 57° to −61°, but those for the NE wind do not have a distinct wide variation range, and it becomes the value such as 22° from 169° to 191°. On the contrary, concerning the maximum values of their wind pressure, those for the SW-wind do not have a distinct variation of wide range, but those for the NE-wind have a distinct variation of range of about 2 times wider.

Table VI shows the time variations of the wind directions for the time durations shown in Figs. 19 and 20, in which are tabulated the following four quantities: (1) the respective long and short axes 2a and

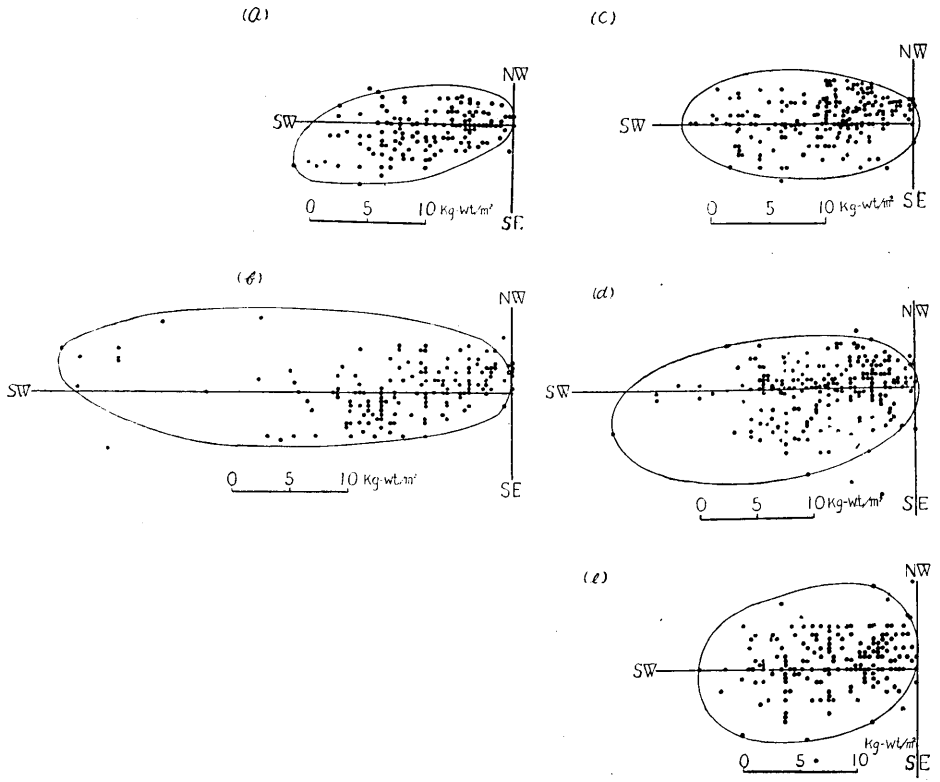


Fig. 20. Relation between wind pressure and wind direction for the NE wind.
(a) 15 h 18 m～15 h 19 m, March 2, 1941,
(b) 16 h 21 m～16 h 22 m, March 2, 1941,
(c) 16 h 22 m～16 h 23 m, March 2, 1941,
(d) 16 h 31 m～16 h 32 m, March 2, 1941,
(e) 17 h 41 m～17 h 42 m, March 2, 1941.

2b of the ellipses shown in Figs. 19 and 20, (2) the angle $\varphi$ between the long axis of the ellipse and the axis of NE-O-SW, (3) the coordinates of $(x, y)$ of the center of the ellipse and also (4) the ratio $b/a$ between the long and short axes 2a and 2b respectively.

Table VI.

| Wind | Date | $2a$ (in kg-wt/m$^2$) | $2b$ (in kg-wt/m$^2$) | $b/a$ | $\varphi$ (in degree) | $x$ (in kg-wt/m$^2$) | $y$ (in kg-wt/m$^2$) |
|---|---|---|---|---|---|---|---|
| SW-wind | $13^h52^m$~$13^h53^m$ | 15.0 | 13.5 | 0.87 | 34 | 6.0 | 1.1 |
| | 13 57 ~13 58 | 25.2 | 12.2 | 0.49 | −80 | 6.0 | 4.2 |
| | 14 0 ~14 1 | 19.5 | 11.1 | 0.57 | 50 | 6.7 | 5.8 |
| | 14 14 ~14 15 $20^s$ | 19.1 | 16.3 | 0.85 | 44 | 8.0 | 2.2 |
| NE-wind | $15^h18^m$~$15^h19^m$ | 19.3 | 8.0 | 0.41 | 190 | 4.5 | 1.1 |
| | 16 21 ~16 22 | 39.0 | 11.7 | 0.30 | 177 | 27.8 | 1.9 |
| | 16 22 ~16 23 | 19.3 | 8.9 | 0.46 | 180 | 9.7 | 0 |
| | 16 31 ~16 32 | 26.6 | 12.3 | 0.46 | 188 | 12.9 | 1.9 |
| | 17 41 ~17 42 | 19.1 | 12.8 | 0.67 | 195 | 8.9 | 0.5 |

From Table VI, we can see that the angle $\varphi$ varies in the greatly wide range 130° from 50° to −80° for the SW-wind and the variation ranges of the angle $\varphi$ for NE wind become from 177° to 195° and they do not have a distinctly wide range such as for the SW-wind. The values of the ratios $b/a$ vary also from 0.49 to 0.87 for the SW-wind and from 0.30 to 0.67 for the NE-wind respectively. From those facts, we can easily understand that the variations of the blowing directions of the SW-wind for a certain time interval have wider range than those of the NE-wind.

## 8. Conclusion and acknowledgement.

Using a new-designed anemometer of inverted pendulum type, we observed the natural winds, and we found that the present apparatus proves useful in the observation of the natural wind.

The analysis results of the records of the natural wind show the complication of the structure of the natural wind, and they confirm the existence of the predominant period of the breath of the wind and the difference of those breath due to the blowing directions of the wind. There are interesting natures for the relations between the breath and the maximum wind pressure and also between the blowing

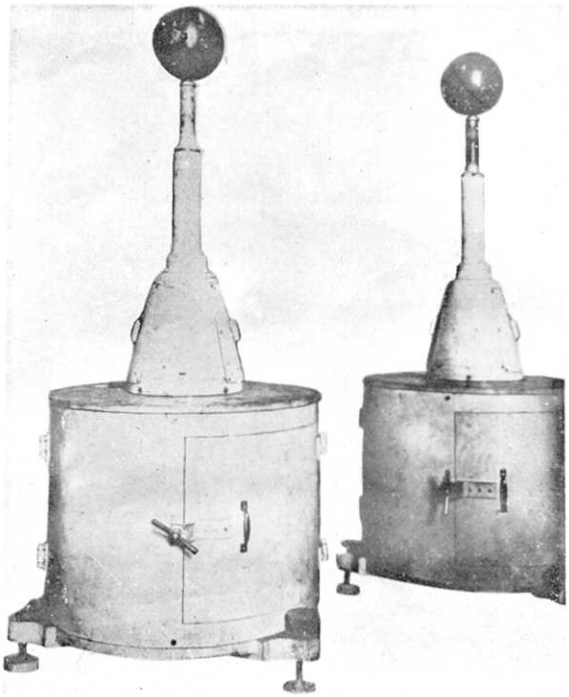

Fig. 2a.

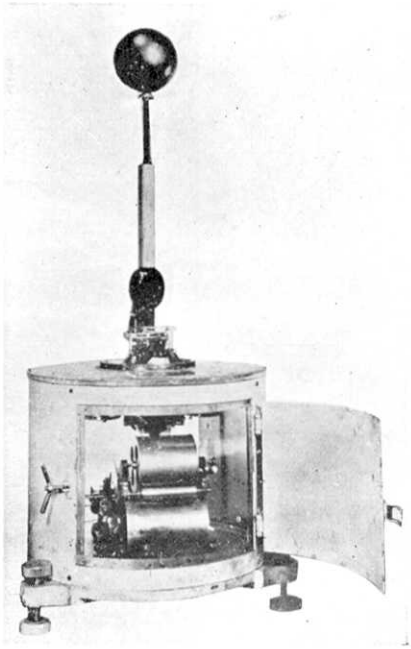

Fig. 2b.

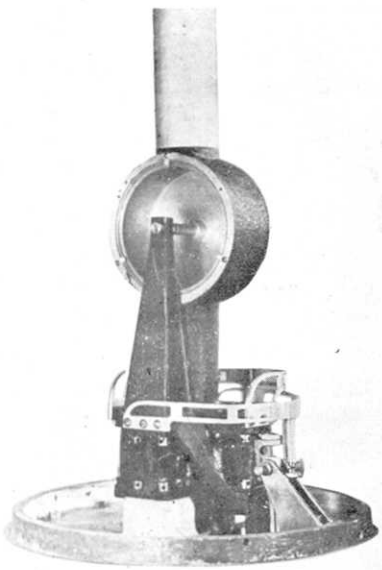

Fig. 2c.

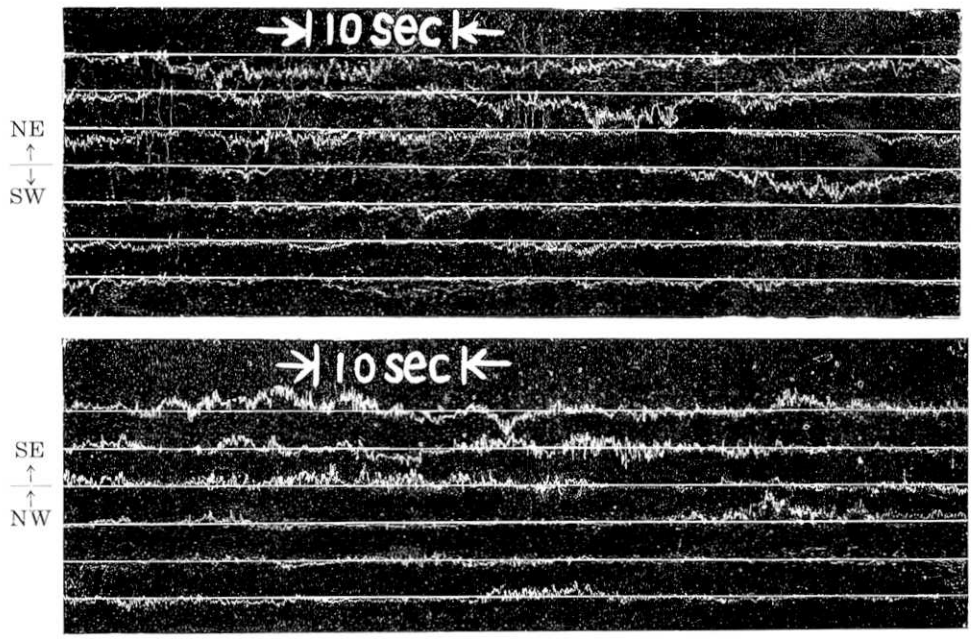


Fig. 11a. Records of natural wind. (14 h, Dec. 2, 1940.)

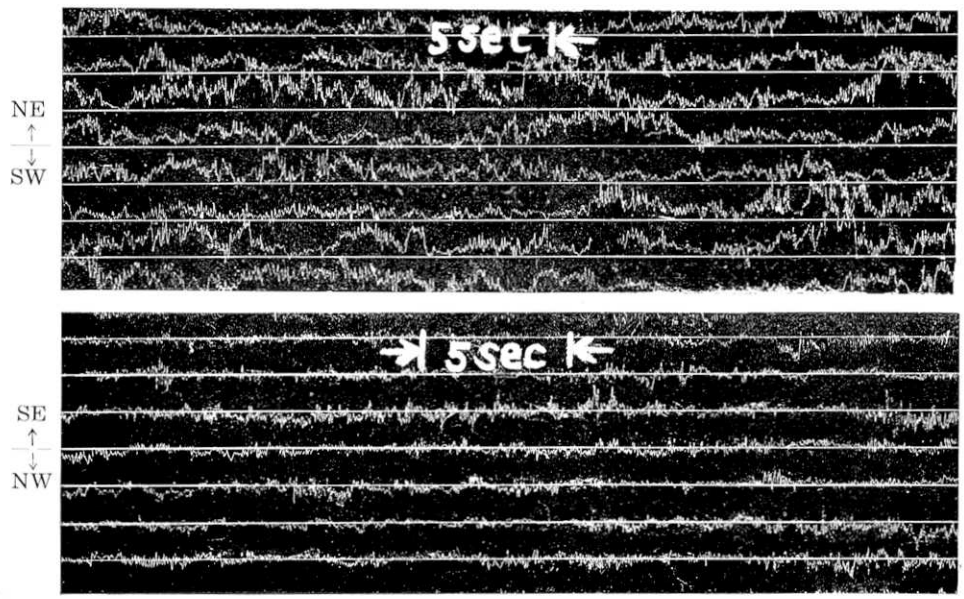


Fig. 11b. Records of natural winds. (13 h, March 2, 1941.)

direction and the wind pressure.

In conclusion, the authors express sincere thanks to the late Mr. Yoshitaro Maeda, by whose enthusiastic assistance in the field observation the present study was carried out. The authors also express hearty thanks to Professor I. Tani who afforded readily facility for using the wind tunnel which belonged to the former Aeronautical Research Institute, Univ. of Tokyo. Lastly the authors express thanks to the authorities of the Institute of the Promotion of Science and Technology of Japan, for appropriating to one of the present writers funds which helped in carrying out the present investigation.

---

## 23. 逆立振子型風力計による自然風の観測と解析

地震研究所 {西村源六郎 / 鈴木正治}

新型自記風力計と本計器を用いて自然風の観測結果の解析を行い，自然風の構造の研究を行った．本計器は逆立振子型自記風力計であって，週期，感度，抵抗係数，槓杆倍率，測定範囲等については次表に示す．

第1表 風力計常数

| 球の直径 | 感度 | 週期 (sec.) | 抵抗係数 (Cx) | 槓杆倍率 | 測定範囲 |
|---|---|---|---|---|---|
| 20 cm | 28.0 kg-wt/m² | 0.075 | 0.48 | 66.5 | 0～20 m/sec |
| 15 cm | 45.5 kg-wt/m² | 0.070 | 0.53 | 66.5 | 0～40 m/sec |

尙制振器は空気制振器であり，記録法は煤煙紙式で，記録用ドラムの駆動は 6 W, 1 r p m の同期電動機により，記録紙速度は 0.4 cm/sec, 0.1 cm/sec, 0.04 cm/sec の三種に変える事が出来，又総重量は約 100 kg-wt, 容積は 80 cm×80 cm×200 cm である．

尙本器の特徴は構造が比較的簡単で丈夫，風圧の瞬時値を精密に記録する事が出来，互に直角な水平二成分を一つの記録用ドラムに記録する事が出来るのでこれを合成する事によって刻々の風向も算出する事が出来る．伊豆稲取町で行った自然風の観測結果の解析によれば，自然風にはその週期即ち息には大体卓越した値が存在すること，また風の方向によってその値が異っており，その最大風圧と息の関係，風圧と風向との関係なども特殊の性質がみられることがわかった．

本計器を用いて自然風についての重要な研究事項，例えば自然風に対する地形の影響，最大風圧と，平均風圧との関係，あるいは週期の持続性の問題，また構造物に対する影響，あるいは脈動に対する影響など，その他種々の研究調査し得べき事項が残されていることは著者等のよくしるところであるが，本報告が自然風の研究者，構造物の設計者，その他この方面に興味をもたられる方に多少でも参考になるところがあれば著者等の幸とするところである．

筆をおくにあたり，著者等の畏敬せる元実業学校教官故前田芳太郎氏の生前における研究に対する御理解によって同氏の家屋を長期間にわたって観測用に用いることができ，同時に同氏の熱心なる観測に対する御援助と御協力とによって全く本研究は遂行し得たものであることを述べ，ことに同氏の霊に感謝する次第である．

なお本研究は日本学術振興会の多大なる援助において遂行し得たものであって，ここに同会に対し感謝の意を表すとともに同会第二特別委員会員である西村に対し各委員が甚大なる御注意及び御指導を下されしことに対し厚く御礼申し上げる次第である．